CHAPTER 3

Instabilities in Linear Accelerators

The wake fields discussed in the previous chapter impose an important limitation on the maximum beam intensity that can be accelerated in a linear accelerator (linac). The limitation is manifested through various collective instabilities when the beam intensity is increased. In Chapter 1, we explained how the direct space charge force imposes intensity limits for proton or heavy ion transport lines. In this chapter, we will investigate the effects of wake fields in general on beam dynamics in a linac. The various linac instabilities mentioned in this chapter are also the basic mechanisms underlying many of the instabilities in circular accelerators to be treated in later chapters.

Compared with their circular counterparts, the wake field effects in a high energy linac do not have the complication of synchrotron motion. The relative longitudinal position of a particle in a beam bunch can be considered to be "frozen." This feature considerably simplifies the linac instability mechanism.

Exercise 3.1

(a) Estimate the relative longitudinal position variations of a particle due to its transverse betatron oscillations. Use $dz/ds \approx -y'(s)^2/2$, where $y(s)$ is the betatron displacement. In the presence of acceleration, $y(s)$ is given by Eq. (3.35). Show that the total change in z due to betatron oscillation is

$$\Delta z \approx -\frac{\hat{y}^2 k_\beta^2 L_0 \gamma_i}{4\gamma_f} \ln \frac{\gamma_f}{\gamma_i}, \tag{3.1}$$

where the symbols are defined in connection with Eq. (3.35).

(b) Estimate the longitudinal position change due to a constant relative energy error $\Delta E/E$. Use

$$\frac{dz}{ds} \approx \frac{1}{\gamma(s)^2} \frac{\Delta E}{E}$$

to show that

$$\Delta z \approx \frac{L_0}{\gamma_i \gamma_f} \frac{\Delta E}{E}. \tag{3.2}$$

(c) Estimate Δz for the SLAC linac, assuming $\gamma_i m_0 c^2 = 1$ GeV, $\gamma_f m_0 c^2 = 50$ GeV, $L_0 = 3$ km, $\hat{y} = 3$ mm, $k_\beta = 0.06$ m^{-1}, and $\Delta E/E = 1\%$. Compare the results with the bunch length, which is of the order of 1 mm.

For some applications, modern linacs are required to perform with increasingly high intensities while maintaining the quality of the beam. One example of such applications is linear colliders for high energy physics experiments. To accelerate particles to TeV energies (1 TeV = 1000 GeV) in a linac requires an extensive length of linac structures, which serve as rf accelerating cavities. To minimize the linac cost and the rf power required, it is desirable to reduce the size of these structures, which generally means strong wake fields. For linear collider applications, one has the challenge that at the end of acceleration, the beam must maintain a small energy spread and a small transverse beam size in spite of these strong wake fields.

In this chapter, the instability mechanisms are often illustrated using a model in which the beam is represented as one or two macroparticles. These macroparticle models give a simple description of the beam dynamics involved. In a *one-particle model*, the beam bunch is a single rigid point charge Ne. The only motion allowed is its center-of-charge motion. In a *two-particle model*, the bunch is represented as two macroparticles separated by a distance $|z|$, which is of the order of the bunch length. Each of the two macroparticles is considered to be a rigid point charge $Ne/2$, whose center of charge is free to move. The two macroparticles interact with the accelerator environment and with each other through the wake fields. These one- and two-particle models will be extended to circular accelerators in Chapter 4.

Three types of linac instabilities are investigated in this chapter, corresponding to the $m = 0$, 1, and 2 components of the wake field, respectively. The $m = 0$ wake causes the parasitic energy loss and an energy spread across the length of the bunch. The parasitic loss effect was discussed in Section 2.5. The energy spread effect is the subject of Section 3.1. Section 3.2 treats the $m = 1$ wake, which causes a dipole mode instability called the *beam breakup* effect in the literature. The $m = 2$ wake, which causes beam breakup in the

quadrupole mode, is the subject of Section 3.3. In all cases, when the beam intensity is sufficiently high, the beam bunch tail will be damaged and perhaps the tail particles will be lost.

3.1 BEAM ENERGY SPREAD

Consider a bunch of charged particles traveling down the accelerator along the axis of the vacuum chamber pipe. The $m = 0$ wake field excited by the beam produces a longitudinal force[1] on particles in the beam. The main effect of this longitudinal force is a retarding voltage, causing energy changes of individual particles. Equations (2.102–2.103) and Section 2.5 address the *total* energy loss of a beam bunch as it traverses an impedance. However, not all particles in the bunch lose the same amount of energy. The wake field thus causes the beam to acquire an energy *spread*, which is the subject of this section.

Consider first a one-particle model in which the beam bunch is a macroparticle of charge Ne that consists of N particles of charge e. As this macroparticle beam travels down the linac, it experiences the self-generated retarding longitudinal field and loses energy accordingly. The parasitic loss per particle is

$$\Delta E = -\tfrac{1}{2}Ne^2W_0'(0^-). \tag{3.3}$$

Take the SLAC linac for example. We have from Figure 2.26(a) that $W_0'(0^-) = 7\ \text{cm}^{-1} \times L_0/L$, where $L_0 = 3$ km is the total length of the linac, and $L = 3.5$ cm is the length of the cavity period. Equation (3.3) then gives an estimate of the parasitic loss of 2.2. GeV for $N = 5 \times 10^{10}$.

This estimate can be improved by using a two-particle model. The beam bunch is then represented by two macroparticles, one leading and another trailing at a distance $|z|$ behind (we have the sign convention $z < 0$). The parasitic loss per particle in the leading macroparticle is half of that for a one-particle model, i.e., 1.1 GeV, because the leading macroparticle contains only half the beam population. The trailing macroparticle loses, in addition to the 1.1 GeV due to self-field, an energy of

$$\Delta E = -\tfrac{1}{2}Ne^2W_0'(z) \tag{3.4}$$

due to the wake field left behind by the leading macroparticle. If we take $z = -\sigma_z = -1$ mm, $N = 5 \times 10^{10}$, and $W_0'(-1\ \text{mm}) = 4.5\ \text{cm}^{-1} \times L_0/L$, each particle in the trailing macroparticle loses an additional 1.4 GeV. The net loss of a trailing particle is therefore 2.5 GeV.

[1] Be reminded that there is no transverse wake force for $m = 0$.

Comparing the one- and the two-particle model results, the one-particle model estimates a parasitic loss per particle of 2.2 GeV; the two-particle model estimates an average loss of $(1.1 + 2.5)/2 = 1.8$ GeV. The results agree reasonably well, but the two-particle model offers the additional information that the wake field has introduced an energy split between the bunch head and the bunch tail, and its magnitude is approximately 1.4 GeV by the time the bunch reaches the end of the linac. If the beam energy at the end of the linac is 50 GeV, this energy spread across the bunch is approximately 3%.

For linear collider applications, this energy spread makes it difficult to focus the beam to a small spot at the collision point in a final focus system, and is to be avoided. Most of this spread can be removed by properly phasing the accelerating rf voltage relative to the beam, as will be discussed in more detail later in this section.

One concern for a high-intensity linear collider can be described as follows. The energy spread at the end of the linac scales as

$$\frac{\Delta E}{E} \approx \frac{\frac{1}{2}Ne^2W_0'}{GL_0} \approx \frac{\frac{1}{2}Ne^2}{Gb^2}, \tag{3.5}$$

where G is the acceleration gradient, and $W_0' \approx L_0/b^2$ is the longitudinal wake function, where b is the vacuum chamber radius characterizing the size of the accelerating cavities. On the other hand, the efficiency of energy extraction by the beam from the field energy U stored in the accelerating cavities $[U \approx (1/8\pi)(G/e)^2 \times \pi b^2 L_0]$ is given by

$$\text{extraction efficiency} \approx \frac{NE}{U} \approx \frac{8Ne^2}{Gb^2}, \tag{3.6}$$

which is equal to 16 times the energy spread (3.5). In other words, to improve the energy spread of the beam at the end of the linac necessarily requires sacrificing the energy extraction efficiency. One way to ameliorate this problem is to compensate $\Delta E/E$ by phasing the rf voltage. Another way is to send a *train* of M bunches per filling of the rf cavities. This will increase the energy extraction efficiency by a factor of M, although at the cost of having to deal with the multibunch interactions due to the long range wake fields.

Exercise 3.2 Even though the transverse wake *force* is zero for $m = 0$, the transverse wake *fields* are not zero. Use Eq. (2.57) to estimate the strengths of E_r and B_θ at the pipe radius $r = b$ for the SLAC linac. Compare the results with the accelerating rf voltage of 600 kV/period.

We now depart from the simplified models and consider a bunch with a general longitudinal distribution $\rho(z)$. The energy change for a test charge e

at longitudinal position z can be written as $eV(z)$, where

$$V(z) = -\int_z^\infty dz'\, \rho(z') W_0'(z - z'). \tag{3.7}$$

A negative $V(z)$ means the test charge loses energy from the wake field. An additional integration of $V(z)$ over the bunch then gives the parasitic loss,

$$\Delta\mathscr{E} = \int_{-\infty}^{\infty} \rho(z) V(z)\, dz. \tag{3.8}$$

For the case of space charge, $V(z)$ can be obtained from Eq. (1.44) [or Eq. (2.80) if one applies Eq. (3.10) below]. For a bunch with Gaussian longitudinal distribution and uniform disk transverse distribution, for example,

$$\frac{V(z)}{L} = \sqrt{\frac{2}{\pi}} \frac{q}{\gamma^2 \sigma_z^2} \left(\ln \frac{b}{a} + \frac{1}{2} \right) f\left(\frac{z}{\sigma_z} \right), \tag{3.9}$$

$$f(u) = u e^{-u^2/2}.$$

Figure 3.1(a) shows the function $f(u)$.

Generally, particles in the front of the bunch ($z > 0$) lose energy due to wake fields, while particles in the back of the bunch ($z < 0$) may gain or lose energy, depending on the length of the bunch. This is not true for the special case of the space charge effect, for which particles in the front of the bunch gain energy, and particles in the back of the bunch lose energy. For the space charge effect, the energy gained by the bunch head is necessarily given up by the bunch tail so that the net energy of the bunch is unchanged.

Consider the numerical example of a 50 MeV proton transport line mentioned following Eq. (1.83). If we take $q = 10^{10}e$, $\sigma_z = 3$ cm, $a = 2$ cm, and $b = 5$ cm, we obtain a longitudinal space charge force of ± 6 V/m for particles located at $z = \pm\sigma_z$. The net energy change of these particles after traveling 100 m of this transport line is $eV/\beta = \pm 2$ keV. The space charge induced beam energy spread is therefore $\pm 4 \times 10^{-5}$.

To calculate $V(z)$ for the resistive wall, it is more convenient to use the frequency domain counterpart of Eq. (3.7), which reads

$$V(z) = -\frac{1}{2\pi} \int_{-\infty}^{\infty} d\omega\, e^{i\omega z/c} Z_0^{\parallel}(\omega) \tilde{\rho}(\omega). \tag{3.10}$$

For a long Gaussian bunch with $\sigma_z \gg \chi^{1/3} b$, we can use the impedance

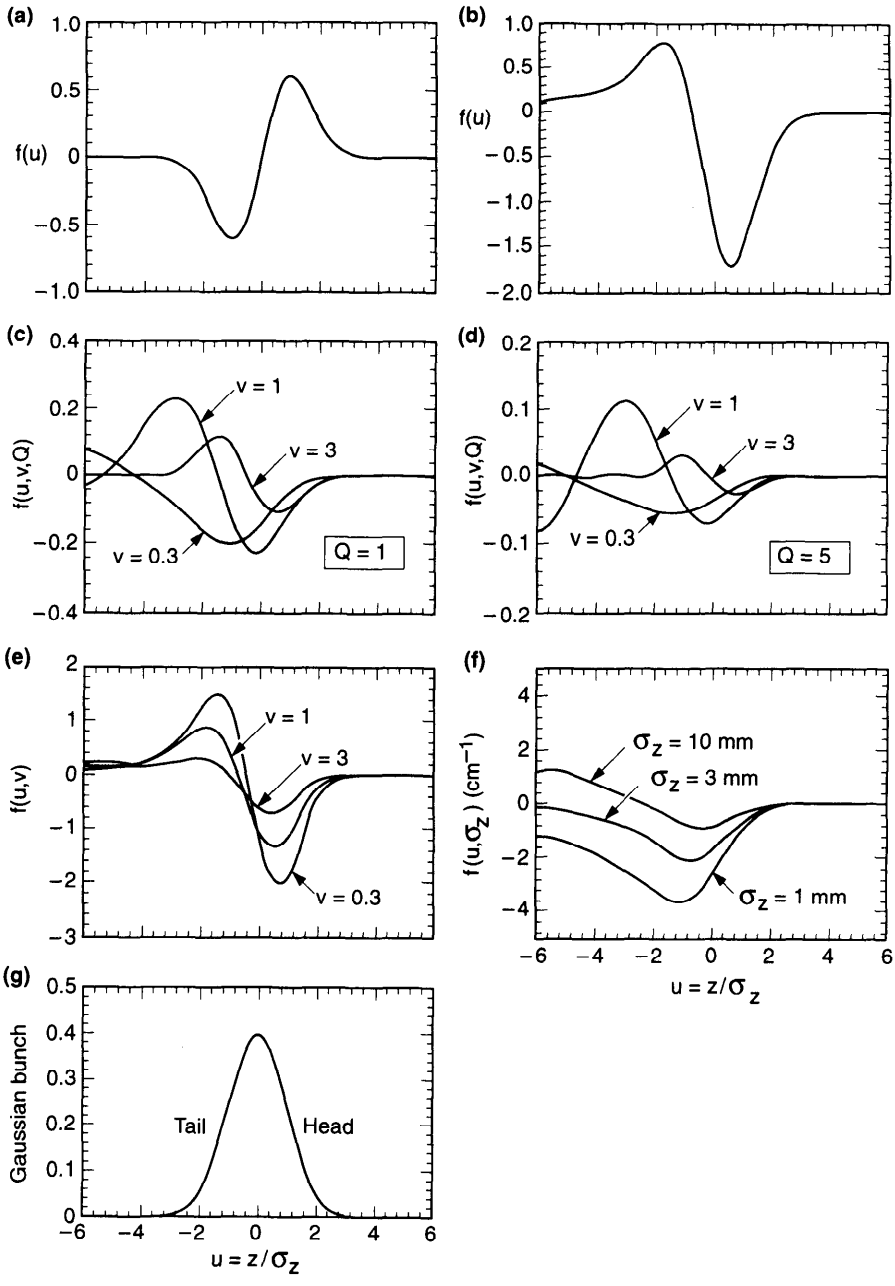

Figure 3.1. (a) The function $f(\upsilon)$ of Eq. (3.9) for the space charge wake effect. (b) The function $f(\upsilon)$ of Eq. (3.11) for the resistive-wall wake. (c) The function $f(\upsilon, v, Q)$ of Eq. (3.14) for a resonator impedance with $Q = 1$ and $v = \omega_R \sigma_z / c = 0.3$, 1, and 3. (d) Same as (c), but for $Q = 5$. (e) The function $f(\upsilon, v)$ of Eq. (3.19) for two parallel plates for $v = L / \sigma_z = 0.3$, 1, and 3. (f) The function $f(\upsilon, \sigma_z)$ of Eq. (3.20) for the SLAC linac for $\sigma_z = 1$, 3, and 10 mm. In all cases, $\upsilon = z / \sigma_z$ and $\upsilon > 0$ is the bunch head. The Gaussian bunch is shown in (g) for reference. All functions f are dimensionless except for part (f).

equation (2.76) to obtain,[2]

$$\frac{V(z)}{L} = \frac{q}{4b\sigma_z^{3/2}}\sqrt{\frac{c}{2\pi\sigma}}\, f\left(\frac{z}{\sigma_z}\right),$$
$$f(u) = -|u|^{3/2}e^{-u^2/4}\left[(I_{-1/4} - I_{3/4})\mathrm{sgn}(u) - I_{1/4} + I_{-3/4}\right] \tag{3.11}$$

with the Bessel functions $I_{\pm 1/4}$ and $I_{\pm 3/4}$ evaluated at $u^2/4$. The function $f(u)$ is shown in Figure 3.1(b).

We continue the above numerical example. Assuming an aluminum pipe and using Figure 3.1(b), a particle located at $0.5\sigma_z$ ahead of bunch center loses an energy of 0.1 eV after traveling 100 m, and a particle located at $1.8\sigma_z$ behind the bunch center gains 0.04 eV.

Exercise 3.3

(a) Integrate Eq. (3.11) over the bunch to recover Eq. (2.194) for the long bunch case.

(b) For a test charge that follows the bunch at a distance $\gg \sigma_z$, i.e., $u \to -\infty$, show that $f(u) \approx \sqrt{8/\pi}|u|^{-3/2}$, and the resulting $V(z)/L$ becomes Eq. (2.16).

(c) Show that, for the resistive-wall wake, a particle at the bunch center loses energy at a rate $2^{3/4}$ times faster than the average in the bunch.

(d) Show that

$$\frac{V'(0)}{L} = -\frac{\Gamma(\frac{1}{4})}{2^{7/4}\pi}\frac{q}{b\sigma_z^{5/2}}\sqrt{\frac{c}{2\pi\sigma}}\,. \tag{3.12}$$

(e) Relate the quantity $V'(0)$ to the synchrotron tune shift in a circular accelerator as discussed following Eq. (1.45) to obtain

$$\Delta\nu_s \approx \frac{\eta R^2}{2\nu_{s0}E}\frac{eV'(0)}{L} = -\frac{\Gamma(\frac{1}{4})}{2^{11/4}\pi}\frac{Nr_0\eta R^2}{\nu_{s0}\gamma b\sigma_z^{5/2}}\sqrt{\frac{c}{2\pi\sigma}}\,. \tag{3.13}$$

For the case of a resonator impedance, we have, using Eq. (3.7),

$$V(z) = \sqrt{\frac{2}{\pi}}\frac{qR_S c}{\sigma_z} f\left(\frac{z}{\sigma_z}, \frac{\omega_R\sigma_z}{c}, Q\right),$$
$$f(u,v,Q) = -\int_0^\infty dx \exp\left[-\frac{1}{2}\left(u + \frac{2Q}{v}x\right)^2 - x\right] \tag{3.14}$$
$$\times\left[\cos\left(x\sqrt{4Q^2-1}\right) - \frac{\sin\left(x\sqrt{4Q^2-1}\right)}{\sqrt{4Q^2-1}}\right].$$

[2]A. Piwinski, DESY Report HERA 92-11 (1992).

The function $f(u, v, Q)$ is shown in Figure 3.1(c) and (d) versus u for various values of v and Q. In the long-bunch limit with $v = \omega_R \sigma_z / c \gg Q$, i.e., when fields decay in a distance $\ll \sigma_z$, we have

$$V(z) \approx -\frac{qR_S c}{\sqrt{2\pi} Q v \sigma_z} \exp\left(-\frac{z^2}{2\sigma_z^2}\right)\left[\frac{1}{Qv}\left(1 - \frac{z^2}{\sigma_z^2}\right) + \frac{z}{\sigma_z}\right]. \quad (3.15)$$

The first term in the square brackets is the resistive contribution; its integration according to Eq. (3.8) gives the parasitic loss (2.198). The second term is a reactive term whose function is to transfer energy from bunch head to bunch tail with no net change of energy for the bunch as a whole. In the long bunch limit, the magnitude of the reactive contribution is larger than the resistive contribution.

If the wake function is written in terms of loss factors according to Eq. (2.148), the retarding voltage of a Gaussian bunch becomes

$$V(z) = -\sqrt{\frac{2}{\pi}} \frac{q}{\sigma_z} \sum_\lambda k_\lambda \int_0^\infty dx \exp\left[-\frac{(z+x)^2}{2\sigma_z^2}\right] \cos\frac{\omega_\lambda x}{c}. \quad (3.16)$$

A test particle at the center of the Gaussian bunch sees a voltage

$$V(0) = -q \sum_\lambda k_\lambda \exp\left(-\frac{\omega_\lambda^2 \sigma_z^2}{2c^2}\right). \quad (3.17)$$

Comparing with the parasitic loss of the entire bunch, Eq. (2.203), we see that the particle at the center of the bunch loses energy faster than average, and that this is true *differentially*, i.e., it holds for each of the individual cavity modes.

For the case of two parallel plates, Eq. (3.16) can be used to obtain $V(z)$ for a Gaussian bunch. The same result can be obtained more readily by using expressions for the wake fields, Eq. (2.171). The result is[3]

$$V(z) = 2 \sum_{n=0}^{\infty} \int_{2nL}^{2(n+1)L} dx\, \rho'(z+x) \ln\left(1 + \frac{2L}{x + 2nL}\right), \quad (3.18)$$

where $\rho'(z)$ is the derivative of ρ. For a Gaussian bunch, we have

$$V(z) = \sqrt{\frac{2}{\pi}} \frac{qL}{\sigma_z^2} f\left(\frac{z}{\sigma_z}, \frac{L}{\sigma_z}\right),$$
$$f(u, v) = \sum_{n=0}^{\infty} \int_{2n}^{2(n+1)} dx (u + xv) e^{-\frac{1}{2}(u+xv)^2} \ln\left(1 + \frac{2}{x + 2n}\right). \quad (3.19)$$

[3]A. Papiernik, M. Chartard-Moulin, and B. Jecko, *Proc. 9th Int. Conf. High Energy Accel.*, SLAC, 1974, p. 375.

Figure 3.1(e) shows the behavior of $f(u, v)$. Integrating Eq. (3.19) over the bunch gives the parasitic loss (2.204–2.205).

For the case of the SLAC linac with loss factors and wake functions shown in Figures 2.25–2.26, we have

$$V(z) = qf\left(\frac{z}{\sigma_z}, \sigma_z\right),$$
$$f(u, \sigma_z) = -\frac{1}{\sqrt{2\pi}} \int_0^\infty dx\, e^{-(x+u)^2/2} W_0'(-x\sigma_z). \tag{3.20}$$

The function $f(u, \sigma_z)$ per cavity period is shown in Figure 3.1(f). Integrating $V(z)$ over the bunch gives Figure 2.33. Note that the sign of the longitudinal wake forces in Figure 3.1, with the exception of the space charge case, is always retarding at the bunch head.

According to Figure 3.1(f), for a bunch with $N = 5 \times 10^{10}$ and $\sigma_z = 1$ mm, a particle located ahead or behind the bunch center by $\sigma_z/2$ loses an energy of 1.2 or 2.1 GeV, respectively. This compares well with the two-particle estimate made at the beginning of this section.

Exercise 3.4 Give expressions for $V(0)$ and $V'(0)$ for the cases of the space charge, the resonator impedance, and the two-parallel-plate cavity. Show that a particle at the bunch center loses more energy than the bunch average by a factor of $2\sqrt{2}$ and 2, respectively, for the resonator and the two-parallel-plate cases in the proper long bunch limits. Given $V'(0)$, compute the incoherent synchrotron tune shift for the various cases. The space charge case gives the same result as Eq. (1.48) for a parabolic bunch if one identifies $\hat{z} = (9\pi/2)^{1/6}\sigma_z$, which is obtained by matching the curvatures of the Gaussian and the parabolic distributions for small z.

In addition to the wake fields, particles in a linac also experience the accelerating rf voltage $V_{\rm rf}(z) = \hat{V}\cos(\omega_{\rm rf} z/c + \phi)$, where $\omega_{\rm rf}$ is the rf angular frequency and ϕ is the phase offset between the bunch center and the rf voltage. (A positive ϕ means the bunch tail gains more energy from the accelerating rf than the bunch head.) The total voltage seen by the beam is $V_{\rm tot}(z) = V_{\rm rf}(z) + V(z)$, where $V(z)$ is the wake field contribution (3.7). To compensate for the wake-induced energy spread, one can adjust the phase offset ϕ at the cost of a slight reduction in the acceleration rate. In particular, one may choose ϕ so that the total voltage in the neighborhood of the bunch center is independent of particle position z, i.e., $V_{\rm tot}'(0) = 0$. This is achieved by choosing ϕ so that

$$\sin\phi = \frac{cV'(0)}{\omega_{\rm rf}\hat{V}}. \tag{3.21}$$

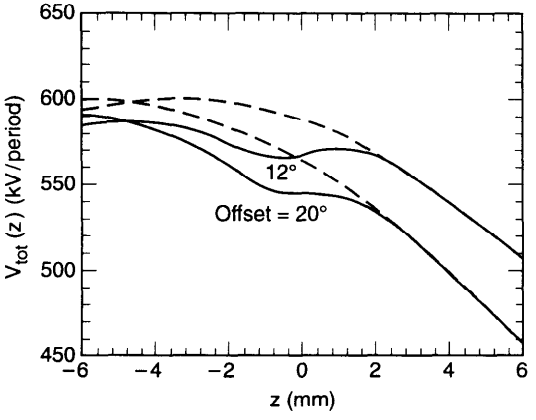

Figure 3.2. Solid curves are the total voltage V_{tot} seen by particles in a SLAC beam with $N = 5 \times 10^{10}$ and $\sigma_z = 1$ mm. Dashed curves are the externally applied rf accelerating voltage with $\hat{V} = 600$ kV / period. Two phase offsets, $\phi = 12°$ and 20°, are shown. The bunch center is at $z = 0$.

Take the SLAC linac with $\sigma_z = 1$ mm, $N = 5 \times 10^{10}$, $\omega_{rf} = 2\pi \times 2.8$ GHz, and $\hat{V} = 600$ kV per cavity period. Using the result from Figure 3.1(f), we find from Eq. (3.21) that $\phi = 20°$. With this choice of phase offset, the acceleration rate at the bunch center is $\hat{V}\cos\phi + V(0) = 545$ kV/period. About $\frac{1}{3}$ of the reduction from 600 kV/period is due to the direct wake field; the remaining $\frac{2}{3}$ is due to the phase offset. By sacrificing beam energy (3 GeV out of 50 GeV), the energy spread between the bunch head and tail is reduced substantially by the phase offset. A compromise between the loss of acceleration rate and reduction of energy spread can be made by choosing a somewhat smaller offset, e.g., 12° instead of 20°. Figure 3.2 shows V_{tot} as a function of z for these two phase offsets.

3.2 BEAM BREAKUP

In the previous section, the beam was considered to be centered in the vacuum chamber pipe. There were no transverse wake forces. In case the beam is off center, for example due to its executing a betatron oscillation,[4] an $m = 1$ dipole wake field will be excited by the head of the bunch, which causes transverse deflection of the tail of the bunch. For a high-intensity beam, the betatron motion of the bunch tail can be seriously perturbed, leading to a transverse breakup of the beam, as will be discussed in this

[4]Dipole wake fields are also excited if the beam is off center for other reasons, such as a misaligned beam trajectory relative to the cavities.

section. The first observation of this beam breakup effect was made on the SLAC linac.[5]

To proceed with a simplified macroparticle model, we first note that a one-particle model is not very useful here, because, unlike the longitudinal $m = 0$ case, a point charge does not exert a transverse wake force on itself. In the two-particle model, the leading macroparticle, unperturbed by its own transverse wake field, executes a free betatron oscillation

$$y_1(s) = \hat{y} \cos k_\beta s, \tag{3.22}$$

where s is the distance coordinate along the linac and k_β is the betatron wave number. The trailing macroparticle, at a distance $|z|$ behind, sees a deflecting wake field left behind by its leading partner. According to Table 2.2, we have

$$\begin{aligned} y_2'' + k_\beta^2 y_2 &= -\frac{Ne^2 W_1(z)}{2EL} y_1 \\ &= -\frac{Nr_0 W_1(z)}{2\gamma L} \hat{y} \cos k_\beta s \end{aligned} \tag{3.23}$$

where $E = \gamma m_0 c^2$ is the beam particle energy, r_0 is the classical radius of the particle [Eq. (1.3)], $W_1(z)$ is the transverse wake function for one cavity period, and L is the cavity period. In writing down Eqs. (3.22–3.23), we have assumed smooth betatron focusing (i.e., k_β is independent of s) and $k_\beta L \ll 1$, so that the wake field can be averaged over cavity periods when describing the particle motion. We have also ignored acceleration of the beam energy in Eq. (3.23). For the SLAC linac, $k_\beta \approx 0.06\ \text{m}^{-1}$ and $k_\beta L \approx 0.002$.

Equation (3.23) shows that the mechanism of beam breakup is that particles in the tail of the beam are driven exactly on resonance by the oscillating wake left by the head of the beam. The solution to Eq. (3.23) is

$$y_2(s) = \hat{y}\left[\cos k_\beta s - \frac{Nr_0 W_1(z)}{4k_\beta \gamma L} s \sin k_\beta s\right], \tag{3.24}$$

in which the first term describes the free oscillation and the second term is the resonant response to the driving wake force. The amplitude of the second term grows linearly with s.

At the end of the linac, the oscillation amplitude of the bunch tail relative to the bunch head is characterized by the dimensionless growth parameter

$$\Upsilon = -\frac{Nr_0 W_1(z) L_0}{4k_\beta \gamma L}, \tag{3.25}$$

[5] R. B. Neal and W. K. H. Panofsky, Science **152**, 1353 (1966); W. K. H. Panofsky and M. Bander, Rev. Sci. Instr. **39**, 206 (1968).

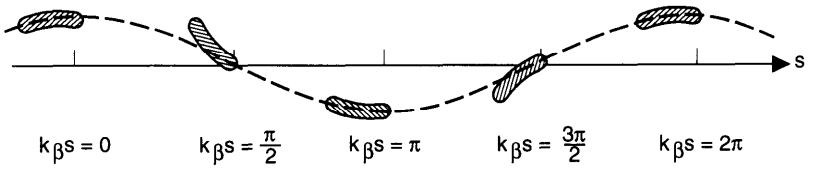

Figure 3.3. Sequence of snapshots of a beam undergoing dipole beam breakup instability in a linac. Values of $k_\beta s$ indicated are modulo 2π. The dashed curves indicate the trajectory of the bunch head.

where L_0 is the total linac length. For short bunches, $W_1(z) < 0$, the parameter Υ is positive.

For a beam bunch with realistic distribution, the wake field due to the off-axis motion of the bunch head deflects the bunch tail so that the bunch is distorted into a banana shape, as sketched in Figure 3.3. The sequence of snapshots shown in Figure 3.3 reflects the fact that the motion of the bunch head is described by $\cos k_\beta s$, while the deviation of the bunch tail relative to the bunch head is described by $s \sin k_\beta s$. In particular, when the bunch head is at a maximum displacement ($k_\beta s = n\pi$), the tail lines up with the bunch head, but when the bunch head displacement is zero [$k_\beta s = (n + \frac{1}{2})\pi$], the tail swing is maximum. As the beam propagates down the linac, the swing amplitude of the flapping tail increases with s until the tail breaks up and particles are lost. Note that the sign of the tail swing shown in Figure 3.3 is not arbitrary, because $\Upsilon > 0$.

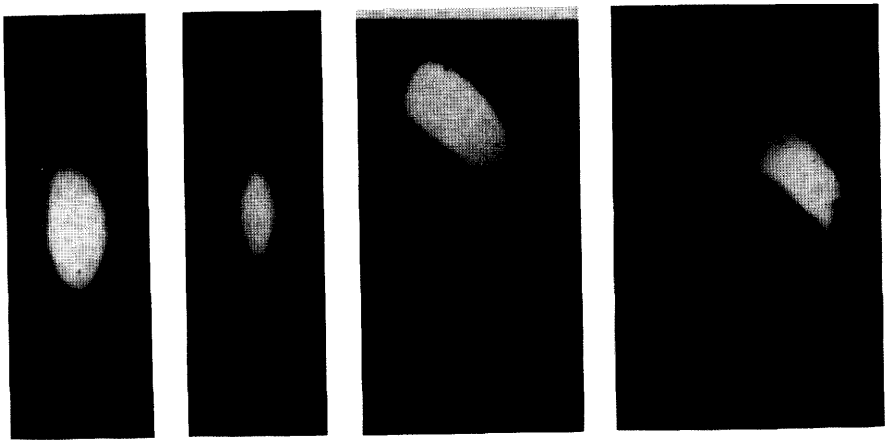

Figure 3.4. Four transverse beam profiles observed at the end of the SLAC linac are shown when the beam was carefully injected and injected with 0.2, 0.5, and 1 mm offsets. The beam sizes σ_x and σ_y are about 120 μm. (Courtesy John Seeman, 1991.)

Figure 3.4 shows four transverse beam profiles observed at the end of the SLAC linac with a beam intensity of $N = 2 \times 10^{10}$.[6] The leftmost profile was observed when the beam was carefully steered so that its trajectory was well centered in the beam pipe. When the beam was injected off center by 0.2, 0.5, and 1 mm, the beam profiles are as shown successively to the right. One observes that a tail develops as the injection offset is increased. The curling of the tail indicates the offset has both horizontal and vertical components.

Consider a beam coasting down the SLAC linac at 1 GeV without acceleration. The tail swing is magnified by a factor of $\Upsilon \approx 180$ compared to the bunch head if we take $N = 5 \times 10^{10}$, $W_1(-1 \text{ mm}) = -0.7 \text{ cm}^{-2}$, $L_0 = 3$ km, $L = 3.5$ cm, and $k_\beta = 0.06 \text{ m}^{-1}$.[7] To preserve the beam emittance, it is necessary to have $|\Upsilon \hat{y}| \ll$ transverse beam size. This means the beam must be injected onto the linac axis with an accuracy better than a fraction of a per cent of the beam size, which is difficult to achieve.

Exercise 3.5 Consider a circular accelerator that has an isochronous design so that it is operated at transition where the slippage factor $\eta = 0$.[8] The longitudinal z-positions of particles are frozen, as in the linac case. Let the accelerator have a broad-band resonator impedance characterized by $\omega_R = c/b$, $Q = 1$, and $Z_0^{\parallel}/n = R_S b/R$, where b is the vacuum pipe radius and $2\pi R$ is the accelerator circumference. Assume the accelerator has a transverse impedance that is related to the longitudinal impedance by Eq. (2.107). Use a two-particle model and Eq. (3.25) to show that if the beam starts with a transverse center-of-charge displacement, the displacement of the bunch tail will double in a time

$$\tau \approx \frac{\gamma b^4 Z_0}{N r_0 c \beta_Z \hat{z} \left(Z_0^{\parallel}/n\right)}, \tag{3.26}$$

where $Z_0 = 377\ \Omega$, $\beta_Z = 1/k_\beta$ is the β-function at the location of the impedance, $\hat{z}$ is the separation of the two macroparticles characterizing the bunch length, and we have assumed a short bunch $\hat{z} \ll b$.

So far we have ignored beam acceleration, which has an important stabilizing effect because, as its energy increases, the beam becomes more rigid and less vulnerable to the wake fields. We will now repeat the two-particle analysis taking account of acceleration. The equation of the free betatron motion for the leading macroparticle is

$$\frac{d}{ds}\left[\gamma(s)\frac{dy_1}{ds}\right] + k_\beta^2 \gamma(s) y_1 = 0, \tag{3.27}$$

where we have assumed that the focusing strength has been increased

[6] J. T. Seeman, K. L. F. Bane, T. Himel, and W. L. Spense, Part. Accel., **30**, 97 (1990).
[7] Strictly speaking, the two-particle model is no longer applicable for a beam broken up so badly.
[8] Claudio Pellegrini and David Robin, Nucl. Instr. Meth. Phys. Res. **A301**, 27 (1991).

proportionally to the beam energy. We further assume a uniform acceleration rate, so that the beam energy increases linearly with s,

$$\gamma(s) = \gamma_i(1 + \alpha s), \tag{3.28}$$

where $\gamma_i m_0 c^2$ is the beam energy at injection. By a change of variable from s to $u = 1 + \alpha s$, Eq. (3.28) becomes

$$\frac{d^2 y_1}{du^2} + \frac{1}{u}\frac{dy_1}{du} + \left(\frac{k_\beta}{\alpha}\right)^2 y_1 = 0. \tag{3.29}$$

The solution with the initial conditions $y_1(0) = \hat{y}$ and $y_1'(0) = 0$ is

$$y_1(u) = \hat{y}\frac{\pi k_\beta}{2\alpha}\left[J_1\left(\frac{k_\beta}{\alpha}\right)N_0\left(\frac{k_\beta}{\alpha}u\right) - N_1\left(\frac{k_\beta}{\alpha}\right)J_0\left(\frac{k_\beta}{\alpha}u\right)\right], \tag{3.30}$$

where $J_n(x)$ and $N_n(x)$ are Bessel and Neumann functions.[9]

The equation of motion for the trailing macroparticle is

$$\frac{d^2 y_2}{du^2} + \frac{1}{u}\frac{dy_2}{du} + \left(\frac{k_\beta}{\alpha}\right)^2 y_2 = -\frac{Nr_0 W_1(z)}{2\gamma_i \alpha^2 L u} y_1(u). \tag{3.31}$$

The solution of Eq. (3.31) can be written as

$$y_2(u) = y_1(u) - \frac{Nr_0 W_1(z)}{2\gamma_i \alpha^2 L}\int_1^u du'\, G(u,u')\, y_1(u'), \tag{3.32}$$

where the first term gives the unperturbed contribution, the second term is the response to the wake force, and $G(u,u')$ is the Green's function

$$G(u,u') = \frac{\pi}{2}\left[N_0\left(\frac{k_\beta}{\alpha}u\right)J_0\left(\frac{k_\beta}{\alpha}u'\right) - J_0\left(\frac{k_\beta}{\alpha}u\right)N_0\left(\frac{k_\beta}{\alpha}u'\right)\right]. \tag{3.33}$$

In most practical cases, the acceleration gradient is much smaller than the betatron focusing, i.e., $\alpha \ll k_\beta$. In this case, the arguments of $J_{0,1}$ and $N_{0,1}$ are much greater than unity, and we can use the asymptotic expressions, for $x \gg 1$,

$$\begin{aligned} J_0(x) &\approx -N_1(x) \approx \sqrt{\frac{2}{\pi x}}\cos\left(x - \frac{\pi}{4}\right), \\ J_1(x) &\approx N_0(x) \approx \sqrt{\frac{2}{\pi x}}\sin\left(x - \frac{\pi}{4}\right). \end{aligned} \tag{3.34}$$

[9]The Bessel functions are complicated in appearance, but not in essence. One could imagine the functions J_n and N_n as the cosine and sine functions expressed in polar coordinates. Similarly, I_n and K_n are like exponential functions expressed in polar coordinates.

This means the motion of the leading macroparticle, Eq. (3.30), is approximately given by

$$y_1(s) \approx \frac{\hat{y}}{\sqrt{1+\alpha s}} \cos k_\beta s, \tag{3.35}$$

and the Green's function (3.33) becomes

$$G(s,s') \approx \frac{\alpha}{k_\beta} \frac{\sin[k_\beta(s-s')]}{\sqrt{(1+\alpha s)(1+\alpha s')}}. \tag{3.36}$$

Compared with the case without acceleration [Eq. (3.22)], Eq. (3.35) contains an extra factor of $1/\sqrt{1+\alpha s}$. This factor can be written as $\sqrt{\gamma_i/\gamma(s)}$, and is the factor responsible for the adiabatic damping of betatron oscillations as particles are accelerated.

Substituting Eqs. (3.35–3.36) into Eq. (3.32) and performing the integration with the approximation $\alpha \ll k_\beta$ gives

$$y_2(s) \approx \frac{\hat{y}}{\sqrt{1+\alpha s}} \left[\cos k_\beta s - \frac{N r_0 W_1(z)}{4 k_\beta \gamma_i \alpha L} \ln(1+\alpha s) \sin k_\beta s \right]. \tag{3.37}$$

At the end of the linac, $s = L_0$, the oscillation amplitude of the bunch tail relative to the bunch head is characterized by the growth parameter

$$\Upsilon = -\frac{N r_0 W_1(z) L_0}{4 k_\beta \gamma_f L} \ln \frac{\gamma_f}{\gamma_i}, \tag{3.38}$$

where $\gamma_f = \gamma_i(1+\alpha L_0) \gg \gamma_i$ gives the final particle energy.

It is interesting to note that the tail growth parameter (3.38) can be obtained from the coasting beam result (3.25) by simply replacing the factor L_0/γ by its integral counterpart $\int_0^{L_0} ds/\gamma(s)$. Due to acceleration, the tail amplitude thus grows logarithmically rather than linearly with s, and the growth parameter is much reduced. If the beam is accelerated in the SLAC linac from 1 to 50 GeV, the factor Υ becomes 14, instead of 180, which was calculated earlier for a beam coasting at 1 GeV.

The beam breakup instability described above is quite severe even with acceleration. To control it, the beam has to be tightly focused, rapidly accelerated, and carefully injected, and its trajectory carefully steered down the linac.[10] It turns out, however, that there is another interesting and

[10] Interestingly, the contribution from trajectory missteering can in principle be largely compensated by an intentional misinjection. See the SLC Linear Collider Conceptual Design Report, SLAC-229 (1980).

effective method to ameliorate the situation. This method, known as the *BNS damping* after Balakin, Novokhatsky, and Smirnov,[11] is described next.

Consider first the case without acceleration, where the leading macroparticle executes a betatron oscillation (3.22). The idea of BNS damping requires introducing a slightly stronger betatron focusing of the bunch tail than the bunch head. The equation of motion of the tail particles can be written as

$$y_2'' + (k_\beta + \Delta k_\beta)^2 y_2 = -\frac{Nr_0 W_1(z)}{2\gamma L}\hat{y}\cos k_\beta s. \tag{3.39}$$

The solution, assuming $|\Delta k_\beta / k_\beta| \ll 1$, is

$$y_2(s) = \hat{y}\cos(k_\beta + \Delta k_\beta)s + \frac{Nr_0 W_1(z)}{4k_\beta \Delta k_\beta \gamma L}\hat{y}\left[\cos(k_\beta s + \Delta k_\beta s) - \cos k_\beta s\right]. \tag{3.40}$$

Compared with Eq. (3.24), one observes that, by introducing a slightly different focusing strength for the bunch tail, the beam breakup mechanism of the bunch head resonantly driving the bunch tail is removed. A further inspection of Eq. (3.40) shows that there exists an interesting condition for the bunch tail to follow the bunch head exactly for all s, namely,

$$\frac{Nr_0 W_1(z)}{4k_\beta \Delta k_\beta \gamma L} = -1, \tag{3.41}$$

or equivalently,

$$\frac{\Delta k_\beta}{k_\beta} = -\frac{Nr_0 W_1(z)}{4k_\beta^2 \gamma L} = \frac{\Upsilon}{k_\beta L_0}, \tag{3.42}$$

where Υ is defined by Eq. (3.25), and $k_\beta L_0$ is the total betatron phase advance of the linac. For short bunches, Υ and Δk_β are positive; the betatron focusing required to fulfill Eq. (3.42) is therefore stronger at the bunch tail than at the bunch head.

Under the BNS condition (3.42), $y_2(s) = y_1(s) = \hat{y}\cos k_\beta s$, and the beam no longer breaks up.[12] Physically, this happens because the additional external focusing force introduced for the bunch tail has compensated for the defocusing dipole deflection force due to the wake field left behind by the

[11] V. Balakin, A. Novokhatsky, and V. Smirnov, *Proc. 12th Int. Conf. High Energy Accel.*, Fermilab, 1983, p. 119.

[12] The mechanism of BNS damping is not to be confused with that of Landau damping, to be discussed in Chapter 5. They have little in common other than the fact that both involve a frequency spread in the bunch population.

bunch head. Note that the BNS focusing has to be adjusted according to the beam intensity.

There are different ways to provide the BNS focusing. One is to introduce a radio frequency quadrupole whose strength changes as the bunch passes by, so that the head and tail of the bunch see different quadrupole strengths. Another is to choose the location of the bunch relative to the acceleration rf voltage in such a way that the bunch tail acquires a lower energy than the bunch head. The energy spread across the bunch then causes a spread in betatron focusing according to

$$\frac{\Delta k_\beta}{k_\beta} = \xi \frac{\Delta E}{E}, \tag{3.43}$$

where ξ is a quantity called the *chromaticity*, which is determined by the linac design. For a FODO lattice design, for example,

$$\xi = -\frac{2}{\mu} \tan \frac{\mu}{2}, \tag{3.44}$$

where μ is the betatron phase advance per FODO cell. By properly choosing the phase of the rf voltage relative to the beam bunch, the betatron focusing required by the BNS condition can be obtained, provided the required $\Delta k_\beta / k_\beta$ is not excessive.

In case of an accelerated beam, the BNS condition is still given by Eq. (3.42), except that the parameter Υ is now that given by Eq. (3.38) instead of Eq. (3.25). Take the SLAC linac, for example, and assume $\mu = 90°$; then the energy deviation of the bunch tail from the bunch head required by the BNS condition is about -5.5%. BNS damping has been routinely employed to control the beam breakup instability in the SLAC linac operations.

Exercise 3.6 The two-particle model analysis can be extended to M particles, and the results can be applied to the case of a train of M equally spaced bunches, each represented as a macroparticle of charge Ne. Let D be the bunch spacing.

(a) In the absence of BNS damping, the kth bunch ($k = 1, 2, \ldots, M$) would have a leading contribution from the wake field that is proportional to N^{k-1}. Show that the betatron displacement of the kth bunch, $y^{(k)}$, is given by the real part of

$$y^{(k)}(s) \approx \frac{\hat{y}}{(k-1)!} \left[\frac{iNr_0 W_1(-D)}{2k_\beta \gamma L} s \right]^{k-1} e^{ik_\beta s}. \tag{3.45}$$

The fact that $y^{(k)} \propto s^{k-1}$ is a consequence of resonant driving of the

kth bunch by the wake field left behind by the $(k-1)$th bunch. For a long train of bunches, the later bunches could therefore be severely perturbed.

(b) One way to control the multibunch beam breakup is to minimize the long range wake fields by a proper design of the accelerating cavities. Show that another way is to apply BNS damping by choosing the focusing strengths for the individual bunches according to[13]

$$\frac{\Delta k_\beta^{(k)}}{k_\beta} = -\frac{Nr_0}{2k_\beta^2 \gamma L} \sum_{j=1}^{k-1} W_1(-jD). \tag{3.46}$$

Does the BNS condition (3.46) apply when different bunches are injected with different initial conditions?

So far we have considered a two-particle model. The beam breakup analysis becomes more involved for a bunch with general distribution $\rho(z)$. Consider first a coasting beam without acceleration. Let $y(s, z)$ be the betatron displacement of a slice of the bunch at longitudinal position z (relative to the bunch center) as it passes the linac coordinate s. The equation of motion of this bunch slice is [assume normalization $\int_{-\infty}^{\infty} dz\, \rho(z) = 1$]

$$y''(s,z) + \left[k_\beta + \Delta k_\beta(z)\right]^2 y(s,z) = -\frac{Nr_0}{\gamma L} \int_z^\infty dz'\, \rho(z') W_1(z - z') y(s, z'). \tag{3.47}$$

In the absence of BNS damping, $\Delta k_\beta(z) = 0$ and the betatron focusing is independent of z. To achieve BNS damping, we would like to have $y(s, z) = \hat{y} \cos k_\beta s$ be the solution of Eq. (3.47) for all values of z. Substituting into Eq. (3.47) yields the condition[14]

$$\frac{\Delta k_\beta(z)}{k_\beta} = -\frac{Nr_0}{2k_\beta^2 \gamma L} \int_z^\infty dz'\, \rho(z') W_1(z - z'). \tag{3.48}$$

Under this condition, there will be no transverse emittance growth due to wake fields. Equation (3.48) is the generalization of the two-particle model result (3.42).

The integral on the right hand side of Eq. (3.48) is also related to the transverse kick received by the beam particles as the beam traverses an impedance with a transverse offset y_0. More specifically, the transverse kick

[13] K. A. Thompson and R. D. Ruth, Phys. Rev. D. **41**, 964 (1990).

[14] V. E. Balakin, *Proc. Workshop on Linear Colliders*, SLAC, 1988, p. 55.

received by a test charge e at position z is

$$\Delta y'(z) = -\frac{Nr_0 y_0}{\gamma}\int_z^\infty dz'\,\rho(z')W_1(z-z'). \tag{3.49}$$

Combining Eqs. (3.48–3.49), the BNS focusing is related to the single-pass wake kick by

$$\Delta k_\beta(z) = \frac{\Delta y'(z)}{2k_\beta y_0 L}. \tag{3.50}$$

Equation (3.49) can also be expressed in terms of the impedance $Z_1^\perp$:

$$\Delta y'(z) = \frac{Nr_0 y_0}{\gamma}\frac{i}{2\pi}\int_{-\infty}^\infty d\omega\, e^{i\omega z/c}Z_1^\perp(\omega)\tilde{\rho}(\omega). \tag{3.51}$$

The kick to the center of charge of the bunch is obtained by integrating $\Delta y'(z)$ over the bunch, yielding

$$\begin{aligned}\langle \Delta y'\rangle &= \int_{-\infty}^\infty dz\,\rho(z)\,\Delta y'(z)\\ &= -\frac{Nr_0 y_0}{\pi\gamma}\int_0^\infty d\omega\,\mathrm{Im}\,Z_1^\perp(\omega)|\tilde{\rho}(\omega)|^2.\end{aligned} \tag{3.52}$$

Note that it is the imaginary part of $Z_1^\perp$ that describes the net kick to the beam. This is in contrast to the net parasitic loss $\Delta\mathscr{E}$, which involves only the real part of $Z_0^\parallel$.

For a Gaussian bunch, we have

$$\begin{aligned}\Delta y'(z) &= \frac{Nr_0 y_0}{\gamma}f\left(\frac{z}{\sigma_z},\sigma_z\right),\\ f(u,\sigma_z) &= -\frac{1}{\sqrt{2\pi}}\int_0^\infty dx\,e^{-(u+x)^2/2}W_1(-x\sigma_z).\end{aligned} \tag{3.53}$$

For the SLAC linac, for example, $W_1(z)$ is that shown in Figure 2.26(b).

When the wake function is expressed in terms of the loss factors as in Eq. (2.166), we have

$$\Delta y'(z) = \sqrt{\frac{2}{\pi}}\frac{Nr_0 y_0 c}{\gamma\sigma_z}\sum_\lambda \frac{k_\lambda^{(1)}}{\omega_\lambda}\int_0^\infty dx\,\exp\left[-\frac{(z+x)^2}{2\sigma_z^2}\right]\sin\frac{\omega_\lambda x}{c}. \tag{3.54}$$

Exercise 3.7 For the space charge wake field (2.55) and a Gaussian bunch, show that

$$\Delta y'(z) = -\sqrt{\frac{2}{\pi}}\frac{NLr_0y_0}{\sigma_z\gamma^3}\left(\frac{1}{a^2}-\frac{1}{b^2}\right)e^{-z^2/2\sigma_z^2}, \tag{3.55}$$

and that $\langle \Delta y' \rangle = \Delta y'(0)/\sqrt{2}$.

Exercise 3.8 For the case of resistive wall, show that[15]

$$\Delta y'(z) = -\frac{NLr_0y_0}{2\gamma b^3}\sqrt{\frac{c}{\pi\sigma\sigma_z}}f\left(\frac{z}{\sigma_z}\right),$$
$$f(u) = |u|^{1/2}e^{-u^2/4}\left[\operatorname{sgn}(u)I_{1/4}\left(\frac{u^2}{4}\right)-I_{-1/4}\left(\frac{u^2}{4}\right)\right]. \tag{3.56}$$

and that

$$\langle \Delta y' \rangle = \frac{\Delta y'(0)}{2^{1/4}} = \frac{NLr_0y_0}{2\pi\gamma b^3}\sqrt{\frac{c}{\pi\sigma\sigma_z}}\Gamma\left(\frac{1}{4}\right). \tag{3.57}$$

Exercise 3.9 For a resonator wake function (2.88), show that

$$\Delta y'(z) = \sqrt{\frac{2}{\pi}}\frac{Nr_0y_0cR_S}{\gamma}f\left(\frac{z}{\sigma_z},\frac{\omega_R\sigma_z}{c},Q\right),$$
$$f(u,v,Q) = \frac{2Q}{v}\int_0^\infty dx\exp\left[-\frac{1}{2}\left(u+\frac{2Q}{v}x\right)^2-x\right] \tag{3.58}$$
$$\times\frac{\sin\left(x\sqrt{4Q^2-1}\right)}{\sqrt{4Q^2-1}}$$

and that, for long bunches with $v = \omega_R\sigma_z/c \gg Q$,

$$\Delta y'(z) \approx \frac{Nr_0y_0cR_S}{\sqrt{2\pi}Qv\gamma}\left(1-\frac{1}{vQ}\frac{z}{\sigma_z}\right)e^{-z^2/2\sigma_z^2}. \tag{3.59}$$

Equations (3.49–3.59) for $\Delta y'(z)$ have their longitudinal counterparts $V(z)$ discussed in the previous section. The various functions defined in those

[15] A. Piwinski, DESY Report 84-097 (1984).

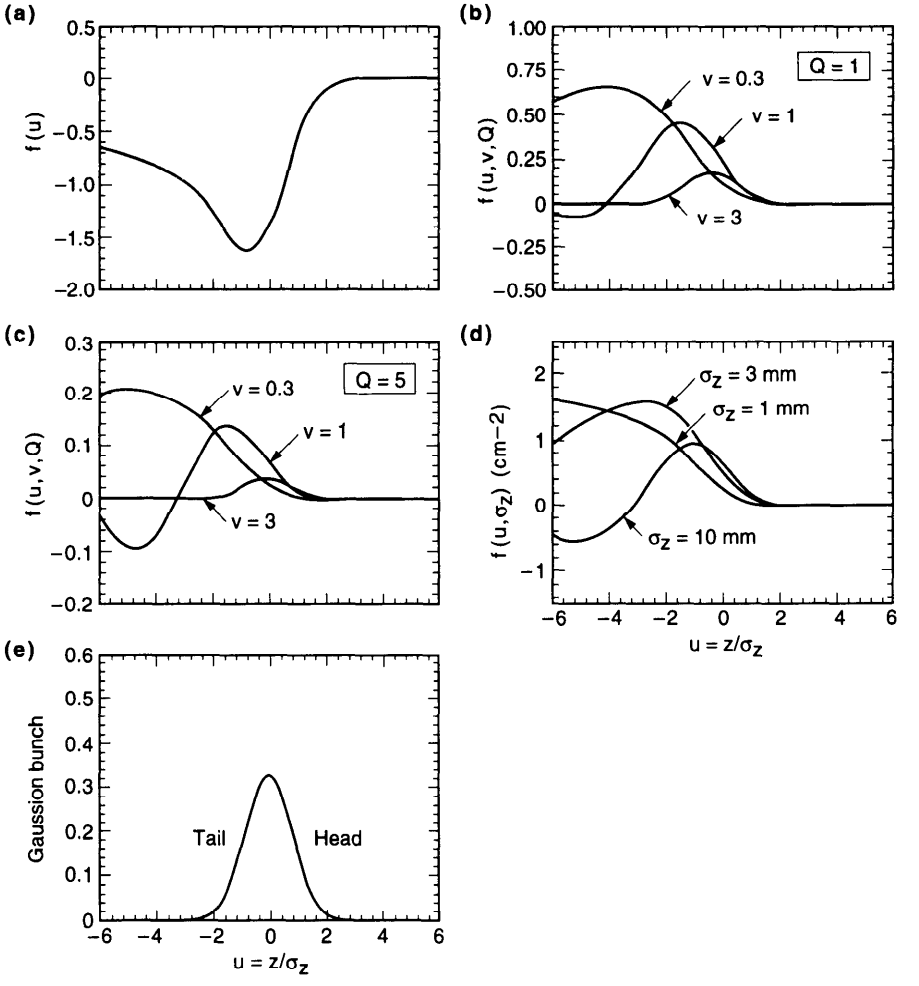

Figure 3.5. (a) The function $f(u)$ of Eq. (3.56) for the resistive-wall impedance. (b) The function $f(u,v,Q)$ of Eq. (3.58) for a resonator impedance with $Q = 1$ and $v = \omega_R \sigma_z / c = 0.3$, 1, and 3. (c) Same as (b), but with $Q = 5$. (d) The function $f(u,\sigma_z)$ of Eq. (3.53) for the SLAC linac, for $\sigma_z = 1$, 3, and 10 mm. In all cases, $u = z / \sigma_z$ and $u > 0$ is the head of the bunch. A Gaussian bunch is shown in (e) for reference.

equations are shown in Figure 3.5. Note that, aside from the space charge case, the sign of $\Delta y'$ tends to be the same as that of y_0 over the bunch population, which reflects the fact that, for an offset beam, the dipole wake field tends to deflect its tail further away from the pipe axis.

As mentioned, with the condition (3.48), the BNS focusing exactly cancels the defocusing effect due to wake fields. In the absence of BNS damping, however, an intense beam can be broken up by the wake fields it generates.

To examine this,[16] let us consider a perturbation expansion

$$y(s, z) = \sum_{n-0}^{\infty} y^{(n)}(s, z), \tag{3.60}$$

where the leading term

$$y^{(0)}(s, z) = \hat{y} \cos k_\beta s \qquad \text{for all } z \tag{3.61}$$

is the unperturbed particle trajectory. The nth term $y^{(n)}$ is $(n-1)$th order in the wake field strength [and therefore $(n-1)$th order in the beam intensity], and is determined by the iteration condition

$$\frac{d^2}{ds^2} y^{(n)}(s, z) + k_\beta^2 y^{(n)}(s, z) = -\frac{Nr_0}{\gamma L} \int_z^\infty dz'\, \rho(z') W_1(z - z') y^{(n-1)}(s, z'). \tag{3.62}$$

The solution to Eq. (3.62) can be expressed in terms of a Green's function $G(s, s') = (1/k_\beta) \sin k_\beta (s - s')$ as

$$y^{(n)}(s, z) = -\frac{Nr_0}{\gamma L} \int_0^s ds'\, G(s, s') \int_z^\infty dz'\, \rho(z') W_1(z - z') y^{(n-1)}(s', z'). \tag{3.63}$$

Equations (3.60), (3.61), and (3.63) give the complete solution to the beam breakup problem in the absence of BNS damping or acceleration. For relatively weak beams, it suffices to keep to the first order term in beam intensity, i.e.,

$$\begin{aligned} y(s, z) &\approx y^{(0)}(s, z) + y^{(1)}(s, z) \\ &= \hat{y}\left[\cos k_\beta s - \frac{Nr_0}{2k_\beta \gamma L} s \sin k_\beta s \int_z^\infty dz'\, \rho(z') W_1(z - z')\right]. \end{aligned} \tag{3.64}$$

This behavior was sketched in Figure 3.3. Note the appearance of the same integral mentioned in conjunction with Eqs. (3.48–3.49). The first order

[16]Analysis of the beam breakup instability under various linac operation and design conditions is a topic much studied in the literature. See R. Helm and G. Loew, *Linear Accelerators*, North Holland, Amsterdam, 1970, Chapter B.1.4; R. F. Koontz, G. A. Loew, R. H. Miller, and P. B Wilson, IEEE Trans. Nucl. Sci. **NS-24**, 1493 (1977); V. K. Neil, L. S. Hall, and R. K. Cooper, Part. Accel. **9**, 213 (1979); Alexander W. Chao, Burton Richter, and Chi-Yuan Yao, *Nucl. Instr. Meth.* **178**, 1 (1980); K. Yokoya, DESY Report 86-084 (1986); T. Suzuki, *AIP Proc.* **156**, *Workshop on Advanced Accel. Concepts*, Madison, 1987, p. 480; Glenn Decker and Jiunn-Ming Wang, Phys. Rev. D **38**, 980 (1988); R. L. Gluckstern, F. Neri, and R. K. Cooper, Part. Accel. **23**, 37 (1988), **23**, 53 (1988); Y. Y. Lau, Phys. Rev. Lett. **63**, 1141 (1989); Yujiro Ogawa, Tetsuo Shidara, and Akira Asami, Phys. Rev. D **43**, 258 (1991).

approximation (3.64) holds if

$$\left| \frac{L_0}{k_\beta} \frac{\Delta y'(z)}{2y_0 L} \right| \ll 1. \tag{3.65}$$

For high intensity beams, the betatron displacement of the beam tail exponentiates with respect to the beam intensity, and we need to include higher order terms in the perturbation expansion. For most practical cases of high energy linacs, the beam executes many betatron oscillations over the length L_0 of the linac, i.e., $k_\beta L_0 \gg 1$. In this case, Eqs. (3.61) and (3.63) can be used to find $y^{(n)}$ at the end of the linac $s = L_0$:

$$y^{(n)}(L_0, z) \approx \frac{\hat{y}}{n!} \left(\frac{iNr_0 L_0}{2k_\beta \gamma L} \right)^n R_n(z) e^{ik_\beta L_0}, \tag{3.66}$$

where taking the real part of the right hand side is understood, and

$$R_n(z) = \int_z^\infty dz_1 \, \rho(z_1) W_1(z - z_1) \int_{z_1}^\infty dz_2 \, \rho(z_2) W_1(z_1 - z_2)$$
$$\cdots \int_{z_{n-1}}^\infty dz_n \, \rho(z_n) W_1(z_{n-1} - z_n) \tag{3.67}$$

with $R_0(z) = 1$.

Exercise 3.10 Consider a beam going through a linac section without betatron focusing. In the absence of wake fields, the beam trajectory is $y(s) = y_0 + y_0' s$. Let the transverse wake function be that given in Eq. (3.70) below.

(a) Use a two-particle model to find the trajectory of the trailing macroparticle.

(b) Solve the general problem following a procedure similar to Eqs. (3.60) and (3.62).

Exercise 3.11 The analysis from Eq. (3.60) to Eq. (3.67) applies also to the case when the external focusing is provided by a solenoid with strength $K = eB_S/E$. The equations of motion are

$$\begin{aligned} x''(s, z) - Ky'(s, z) &= -\frac{Nr_0}{\gamma L} \int_z^\infty dz' \, \rho(z') W_1(z - z') x(s, z'), \\ y''(s, z) + Kx'(s, z) &= -\frac{Nr_0}{\gamma L} \int_z^\infty dz' \, \rho(z') W_1(z - z') y(s, z'). \end{aligned} \tag{3.68}$$

Observe the beam motion in a rotating frame by defining

$$u = e^{iKs/2}(x + iy).$$

Show that

$$u''(s,z) + \frac{K^2}{4}u(s,z) = -\frac{Nr_0}{\gamma L}\int_z^\infty dz'\,\rho(z')W_1(z-z')u(s,z'). \quad (3.69)$$

The analysis in the text then applies straightforwardly.

To proceed, let us consider the special case in which the bunch distribution is uniform with total length l and the wake function is linear in z, i.e.,

$$\begin{aligned} \rho(z) &= \begin{cases} 1/l & \text{if} \quad |z| < l/2, \\ 0 & \text{otherwise}, \end{cases} \\ W_1(z) &= \frac{W_0 z}{l} \qquad \text{if} \quad 0 > z > -l. \end{aligned} \quad (3.70)$$

In this parametrization, W_0 is necessarily positive. We find from Eq. (3.67),

$$R_n(z) = \frac{1}{(2n)!}\left[-NW_0\left(\frac{1}{2} - \frac{z}{l}\right)^2\right]^n, \qquad |z| < \frac{l}{2}. \quad (3.71)$$

Equations (3.60) and (3.66) then give

$$y(L_0,z) = \hat{y}e^{ik_\beta L_0}\sum_{n=0}^{\infty}\frac{1}{n!(2n)!}\left(\frac{\Upsilon}{2i}\right)^n, \quad (3.72)$$

where we have defined a dimensionless wake strength parameter

$$\Upsilon = \frac{Nr_0L_0W_0}{k_\beta\gamma L}\left(\frac{1}{2} - \frac{z}{l}\right)^2. \quad (3.73)$$

The parameter Υ depends on the location z within the beam bunch. At the bunch head $z = l/2$, we have $\Upsilon = 0$. At the bunch tail $z = -l/2$, Υ has its maximum value. For $\Upsilon \ll 1$, we have the condition (3.65), and Eq. (3.64) is recovered from Eq. (3.72). In the limit $\Upsilon \gg 1$, Eq. (3.72) has the following

asymptotic expression:[17]

$$y(L_0, z) \approx \frac{\hat{y}}{\sqrt{6\pi}} \Upsilon^{-1/6} \exp\left(\frac{3^{3/2}}{4}\Upsilon^{1/3}\right)\cos\left(k_\beta L_0 - \frac{3}{4}\Upsilon^{1/3} + \frac{\pi}{12}\right). \tag{3.74}$$

The bunch tail thus breaks up exponentially with an exponent proportional to $\Upsilon^{1/3}$.

In case the beam is being accelerated in the linac, the result (3.74) still applies provided we replace $\hat{y}$ by the adiabatically damped value $\hat{y}\sqrt{\gamma_i/\gamma_f}$, where $\gamma_{i,f}m_0c^2$ are the initial and final particle energies, and the factor L_0/γ in the expression (3.73) by its average value $(L_0/\gamma_f)\ln(\gamma_f/\gamma_i)$. These substitution rules have been discussed following Eq. (3.38) in connection with the two-particle model.

For the SLAC linac, we may take $W_0 = 1.4$ cm^{-2}, $L = 3.5$ cm, $L_0 = 3000$ m, $N = 5 \times 10^{10}$, $\gamma_i = 2 \times 10^3$, $\gamma_f = 10^5$, $k_\beta = 0.06$ m^{-1}, and $\alpha = 0.016$ m^{-1}, and obtain $\Upsilon = 115$ at the very tail of the uniform bunch for the accelerated beam. For the case of a beam coasting at 1 GeV, we have $\Upsilon = 1400$ at the bunch tail. Figure 3.6(a) shows the snapshots of an accelerated beam as it approaches the end of the linac. The coasting beam snapshots are shown in Figure 3.6(b). For relatively weak beams, the corresponding beam behavior was illustrated in Figure 3.3.

Exercise 3.12 Consider a uniform bunch as in Eq. (3.70) but a constant wake $W_1(z) = -W_0$ ($W_0 > 0$). Show that

$$y(L_0, z) \approx \hat{y}e^{ik_\beta L_0} I_0\left(\sqrt{-2i\Upsilon}\right),$$
$$\Upsilon = \frac{Nr_0 L_0 W_0}{k_\beta \gamma L}\left(\frac{1}{2} - \frac{z}{l}\right), \tag{3.75}$$

where $I_0(x)$ is the Bessel function. For $\Upsilon \gg 1$, show that

$$y(L_0, z) \approx \frac{\hat{y}}{2^{3/4}\pi^{1/2}} \Upsilon^{-1/4} e^{\sqrt{\Upsilon}} \cos\left(k_\beta L_0 - \sqrt{\Upsilon} + \frac{\pi}{8}\right). \tag{3.76}$$

[17]The derivation of Eq. (3.74), omitted here, can be obtained by the method of steepest descents. This mathematical technique follows from the observation that the summation in Eq. (3.72) involves terms that are products of a rapidly rising function of n, namely Υ^n, and a rapidly diminishing function of n, namely $1/n!(2n)!$. The summation is therefore over a sharply peaked function of n. The method of steepest descents, which basically means fitting this sharply peaked function with a Gaussian and approximating the summation by the area under the Gaussian, can be applied to yield Eq. (3.74).

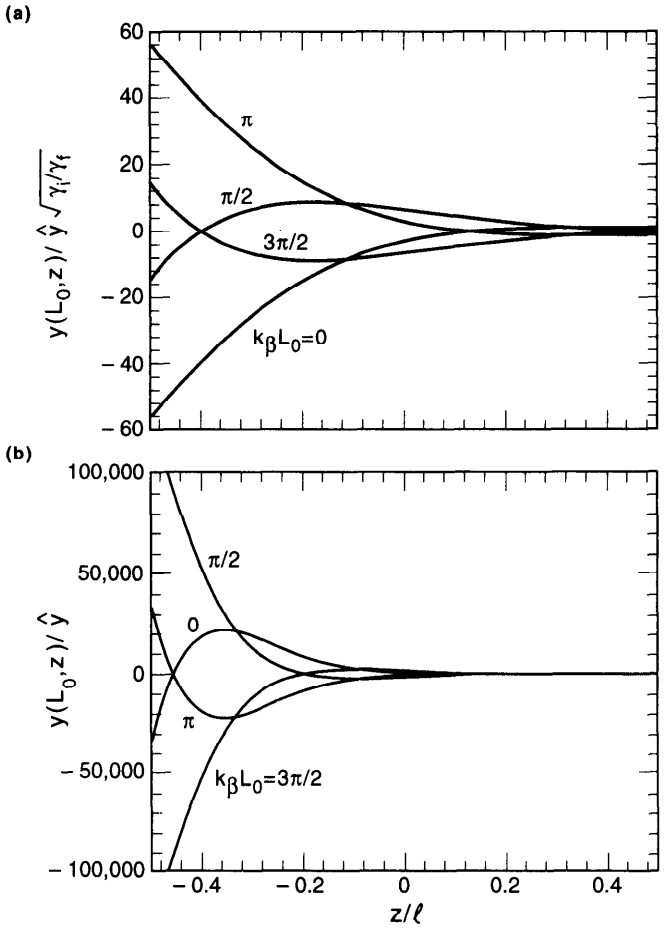

Figure 3.6. Bunch distortion due to dipole beam breakup for the case when the beam distribution and the wake function are described by Eq. (3.70). Four snapshots are shown with $k_\beta s$ (modulo 2π) $= 0, \pi/2, \pi$, and $3\pi/2$ towards the end of the linac. The wake strength parameter at the bunch tail is (a) $\Upsilon = 115$ for an accelerated beam, and (b) $\Upsilon = 1400$ for a coasting beam.

Exercise 3.13 Consider a uniform bunch and a resistive-wall wake $W_1(z) = -W_0\sqrt{-l/z}$. Show that

$$y(L_0, z) \approx \hat{y} e^{ik_\beta L_0} \sum_{m=0}^{\infty} \left(-\frac{\pi\Upsilon^2}{4}\right)^m \times \left[\frac{1}{m!(2m)!} - i\frac{2^m\Upsilon}{(2m+1)!!(2m+1)!}\right], \quad (3.77)$$

$$\Upsilon = \frac{Nr_0L_0W_0}{k_\beta\gamma L}\sqrt{\frac{1}{2} - \frac{z}{l}}\,.$$

So far we have been considering the transverse effects of the $m = 1$ wake fields. It should be remembered that this same transverse dipole wake force also has a longitudinal partner that affects the beam energy spread. If the beam is injected off center into a linac, in addition to a transverse deflecting wake force connected with $W_1(z)$, it also generates a dipole longitudinal wake force connected with $W_1'(z)$. To illustrate this, let us again consider a two-particle model with a leading macroparticle of charge $Ne/2$ with displacement y_1 and a trailing macroparticle, which is a distance $|z|$ behind and has a displacement y_2. A particle in the trailing macroparticle sees, in addition to a transverse wake potential $-Ne^2W_1(z)y_1/2$, a longitudinal wake potential

$$\Delta E = -\tfrac{1}{2}Ne^2W_1'(z)y_1y_2. \tag{3.78}$$

A consequence of this longitudinal wake is to cause an energy spread in the beam that depends on both the longitudinal and transverse positions of the particle. In contrast, the $m = 0$ wake force produces an energy spread that depends only on the longitudinal position of the particle under consideration.

If the beam displacement comes from an injection error, and if the transverse wake fields are ignored, we have $y_1 = y_2 = (\hat{y}\cos k_\beta s)/\sqrt{1 + \alpha s}$. It follows by integrating Eq. (3.78) over the linac that

$$\Delta E \approx -\frac{1}{4}Ne^2\hat{y}^2W_1'(z)\frac{\gamma_i}{\gamma_f}\ln\frac{\gamma_f}{\gamma_i}. \tag{3.79}$$

Equation (3.79) can be compared with the energy spread caused by the $m = 0$ wake, Eq. (3.4). Since W_0'/W_1' is of the order of b^2, where b is the vacuum chamber pipe radius, the energy loss due to the $m = 0$ wake is typically much larger than that due to the $m = 1$ wake if the transverse beam displacement $|y| \ll b$. For the SLAC linac, if we take $W_1'(-1\text{ mm}) = 6\text{ cm}^{-3} \times L_0/L$, cavity period $L = 3.5$ cm, $\hat{y} = 1$ mm, $N = 5 \times 10^{10}$, $\gamma_f/\gamma_i = 50$, and a total linac length of $L_0 = 3$ km, the energy loss of a particle in the trailing macroparticle due to this effect is 0.7 MeV.

3.3 QUADRUPOLE BEAM BREAKUP

The next topic to be discussed is the transverse *quadrupole beam breakup instability* ($m = 2$) in a linac. This instability becomes significant when the transverse beam size is comparable to the beam pipe radius b. What happens then is that the quadrupole wake field generated by the bunch head perturbs the focusing force on the bunch tail, leading to an instability if the beam is sufficiently intense. Unlike the dipole beam breakup instability, this $m = 2$ effect does not have to originate from injection or alignment errors. As we will soon see, a well-steered beam can be broken up by the $m = 2$ wake forces.

Consider a beam bunch whose trajectory in a linac is centered in the vacuum chamber pipe so that no dipole wake fields are generated. Quadrupole wake fields, however, can be generated if the transverse beam shape is not round, in which case the beam possesses two types of quadrupole moments, one normal and one skewed:

$$Q_n = \langle x^2 \rangle - \langle y^2 \rangle \quad \text{and} \quad Q_s = 2\langle xy \rangle, \tag{3.80}$$

where the brackets indicate averaging over the transverse bunch distribution.

Consider a beam represented as an elliptically shaped slice of charge q and quadrupole moments Q_n and Q_s. Quadrupole wake fields are generated behind this beam slice. A test charge e that trails the beam slice at a distance $|z|$ $(z < 0)$ would see a transverse wake force

$$\vec{F}_\perp = -2eq\frac{W_2(z)}{L}\left[Q_n(x\hat{x} - y\hat{y}) + Q_s(y\hat{x} + x\hat{y})\right], \tag{3.81}$$

where $W_2(z)$ is the quadrupole wake function of the linac for one cavity period and L is the cavity period length. The wake force due to Q_n resembles the force seen by a particle as it traverses a quadrupole magnet, and the wake force due to Q_s resembles that of a skew quadrupole magnet.

For a beam bunch with total charge Ne and longitudinal distribution $\rho(z)$, a particle located at a position z relative to the bunch center sees the quadrupole wake fields left behind by all charge slices in front of it. These wake fields are equivalent to that of a quadrupole magnet of strength

$$\frac{1}{B\rho}\frac{\partial B_y}{\partial x} = \frac{1}{B\rho}\frac{\partial B_x}{\partial y} = \frac{2Nr_0}{\gamma L}\int_z^\infty dz'\,\rho(z')W_2(z - z')Q_n(z'), \tag{3.82}$$

and a skew quadrupole magnet of strength

$$\frac{1}{B\rho}\frac{\partial B_y}{\partial y} = -\frac{1}{B\rho}\frac{\partial B_x}{\partial x} = \frac{2Nr_0}{\gamma L}\int_z^\infty dz'\,\rho(z')W_2(z - z')Q_s(z'), \tag{3.83}$$

where $1/B\rho = e/E$ is the beam rigidity. In the following, we assume the transverse beam distribution is upright in the x-y plane, so that the skew moment $Q_s = 0$.

There are two main sources of the normal quadrupole moments of the beam distribution. The first comes from the fact that the beam sizes $\langle x^2 \rangle$ and $\langle y^2 \rangle$ scale with the β-functions β_x and β_y, respectively. In a FODO lattice, for example, β_x and β_y alternate their maximum and minimum values along the accelerator, giving rise to a nonvanishing Q_n that oscillates with a period equal to the FODO cell length. The second source of

quadrupole moment results from injecting a beam whose beam size at the injection point does not match that prescribed by the linac lattice.

The first source is there even in an ideal operation. Instability occurs when the phase advance per FODO cell, μ, is close to 180°. However, even if μ is away from 180° so that the motion of the bunch tail is stable, the quadrupole wake fields can distort the tail distribution and cause an effective increase of the beam emittance. The second source is a result of operation errors. Its corresponding quadrupole moment, and thus the wake force, oscillates with twice the betatron oscillation frequency. Such an oscillation resonantly drives the particles in the bunch tail, leading to a beam breakup instability just like the dipole beam breakup mechanism. Effects of both sources of quadrupole moments are discussed below.

Consider a FODO lattice, and a beam with equal horizontal and vertical emittances $\epsilon_x = \epsilon_y = \epsilon(s)$. Identifying $\langle x^2 \rangle = \epsilon_x \beta_x$ and $\langle y^2 \rangle = \epsilon_y \beta_y$, the quadrupole moment at position s is given by

$$Q_n(s) = \epsilon(s)\big[\beta_x(s) - \beta_y(s)\big]. \tag{3.84}$$

With acceleration, the beam energy and emittance are given by

$$\gamma(s) = \gamma_i(1 + \alpha s) \quad \text{and} \quad \epsilon(s) = \frac{\epsilon_i}{1 + \alpha s}, \tag{3.85}$$

where γ_i and ϵ_i are the quantities at the injection point of the linac.

The quadrupole wake force induces a perturbation of the betatron phase advances, ψ_x and ψ_y, on particles in the bunch tail. When μ is sufficiently away from 180°, these phase advance perturbations, accumulated over the length L_0 of the linac, are given by

$$\begin{aligned}\Delta\psi_{x,y} &= \pm\frac{1}{2}\int_0^{L_0} ds\, \beta_{x,y}\left(\frac{1}{B\rho}\frac{\partial B_y}{\partial x}\right) \\ &= \pm\frac{Nr_0\epsilon_i}{\gamma_i L}\int_z^{\infty} dz'\,\rho(z')W_2(z - z')\int_0^{L_0} ds\,\frac{\beta_{x,y}(s)\big[\beta_x(s) - \beta_y(s)\big]}{(1 + \alpha s)^2},\end{aligned} \tag{3.86}$$

where the upper and lower signs are for $\Delta\psi_x$ and $\Delta\psi_y$, respectively.

If acceleration is slow, so that the particle energy does not vary significantly over a FODO cell, we can approximate the quantity $\beta_{x,y}(\beta_x - \beta_y)$ in the integrand of Eq. (3.86) by their average values over a FODO cell,

$$\big\langle \beta_{x,y}(s)\big[\beta_x(s) - \beta_y(s)\big]\big\rangle = \pm\frac{L_c^2}{6\cos^2(\mu/2)}, \tag{3.87}$$

where L_c is the FODO cell length. The divergence at $\mu = 180°$ is evident.

Substituting Eq. (3.87) into Eq. (3.86) gives

$$\Delta\psi_x \approx \Delta\psi_y \approx \frac{Nr_0\epsilon_i L_c^2}{6\gamma_i \alpha L \cos^2(\mu/2)} \int_z^\infty dz'\, \rho(z') W_2(z - z'). \quad (3.88)$$

For short bunches, the integral in Eq. (3.88) and thus the betatron phase perturbation $\Delta\psi_{x,y}$ are negative. This reflects the fact that the quadrupole wake force tends to *defocus* on bunch tail.

In some applications, such as for a free electron laser or a linear collider, it is important to avoid emittance growths. Since the betatron phase advances at the bunch head and tail are different, there is a significant growth of the effective emittance if $|\Delta\psi_{x,y}| \gtrsim 1$.

With a two-particle model (actually a two-slice model), the tail slice has a phase advance perturbation

$$\Delta\psi_{x,y} \approx \frac{Nr_0\epsilon_i L_c^2 W_2(z)}{12\gamma_i \alpha L \cos^2(\mu/2)}. \quad (3.89)$$

If $N = 5 \times 10^{10}$, $\epsilon_i = 1.5 \times 10^{-8}$ m, $L_c = 25$ m, $W_2(-1\text{ mm}) = -0.4\text{ cm}^{-4}$, $\mu = 90°$, $\alpha = 0.016\text{ m}^{-1}$, and $L = 3.5$ cm, we obtain $\psi_{x,y} \approx -8$ mrad.

This type of quadrupole beam breakup can be avoided if solenoids are used instead of quadrupole magnets for focusing, in which case the transverse beam shape can be made round. It is also possible to avoid it by the equivalent of a BNS damping. This can be achieved by adjusting the betatron focusing along the length of the bunch according to

$$\Delta k_\beta(s, z) \approx -\frac{Nr_0\epsilon(s) L_c^2}{6\gamma(s) L \cos^2(\mu/2)} \int_z^\infty dz'\, \rho(z') W_2(z - z') \quad (3.90)$$

to compensate for the wake induced perturbation (3.88).

To illustrate the second quadrupole beam breakup mechanism, we consider a two-slice model consisting of two elliptically shaped thin slices of charge $Ne/2$ each.[18] Consider for simplicity a coasting beam which by design has a round transverse beam distribution with $\langle x^2\rangle = \langle x'^2\rangle/k_\beta^2 = \langle y^2\rangle = \langle y'^2\rangle/k_\beta^2 = a^2$, where k_β is the betatron wave number, assumed uniform along the linac and equal in the x and y planes. Assume the beam is injected with an error in the horizontal beam size with $\langle x^2\rangle = a^2(1 + \Delta)$ and $\langle x'^2\rangle/k_\beta^2 = a^2(1 - \Delta)$, where $|\Delta| \ll 1$ is an error parameter.

The beam sizes of the leading particle slice behave according to

$$\langle x^2\rangle = a^2 + a^2\Delta \cos 2k_\beta s \quad \text{and} \quad \langle y^2\rangle = a^2. \quad (3.91)$$

[18]A one-slice model would not be very useful, because the slice would not see its own transverse wake force.

The vertical beam size is unperturbed, and the horizontal beam size oscillates with twice the betatron frequency. The quadrupole moment of the leading slice is given by $Q_n = \langle x^2 \rangle - \langle y^2 \rangle = a^2\Delta \cos 2k_\beta s$.

In the absence of BNS damping, a test charge e in the trailing particle slice is driven resonantly by the quadrupole wake field left behind by the leading slice according to[19]

$$\begin{aligned} x'' + k_\beta^2 x &= -\frac{Nr_0 W_2(z) a^2 \Delta}{\gamma L} x \cos 2k_\beta s, \\ y'' + k_\beta^2 y &= \frac{Nr_0 W_2(z) a^2 \Delta}{\gamma L} y \cos 2k_\beta s. \end{aligned} \tag{3.92}$$

For a modestly strong beam, Eq. (3.92) can be solved by iteration, keeping only the resonant contributions, to yield

$$\begin{aligned} x &\approx x_0 \cos k_\beta s + \frac{x_0'}{k_\beta} \sin k_\beta s \\ &\quad - \frac{Nr_0 W_2(z) a^2 \Delta}{4k_\beta \gamma L} s \left[x_0 \sin k_\beta s + \frac{x_0'}{k_\beta} \cos k_\beta s \right], \\ y &\approx y_0 \cos k_\beta s + \frac{y_0'}{k_\beta} \sin k_\beta s \\ &\quad + \frac{Nr_0 W_2(z) a^2 \Delta}{4k_\beta \gamma L} s \left[y_0 \sin k_\beta s + \frac{y_0'}{k_\beta} \cos k_\beta s \right]. \end{aligned} \tag{3.93}$$

The wake field term is proportional to s, indicating the bunch tail is resonantly driven.

We are interested in the rms beam size of the trailing slice, which is given by

$$\begin{aligned} \langle x^2 \rangle &\approx a^2 + a^2 \Delta \cos 2k_\beta s - \frac{Nr_0 W_2(z) a^4 \Delta}{2k_\beta \gamma L} s \sin 2k_\beta s, \\ \langle y^2 \rangle &\approx a^2 + \frac{Nr_0 W_2(z) a^4 \Delta}{2k_\beta \gamma L} s \sin 2k_\beta s. \end{aligned} \tag{3.94}$$

The behavior of these two particle slices is sketched in Figure 3.7. The

[19]These are special cases of Mathieu's equation.

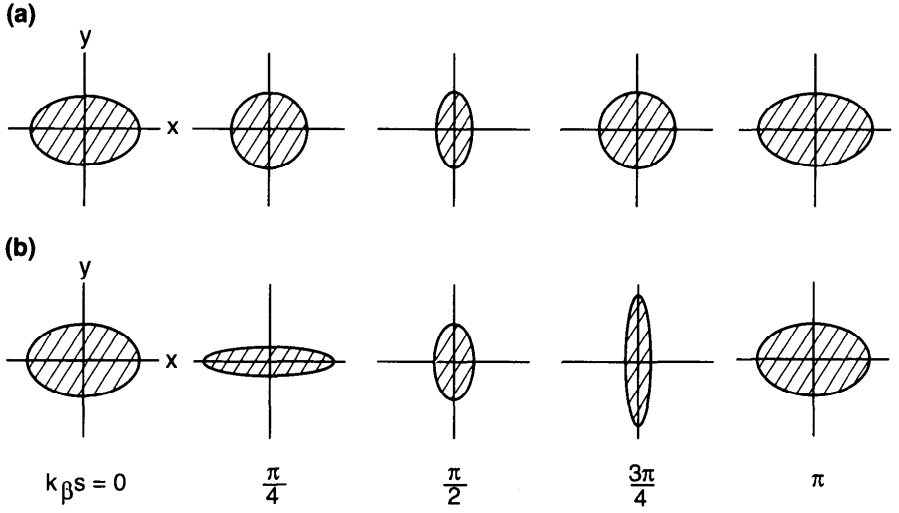

Figure 3.7. Snapshots of the beam shape when the bunch is injected with a mismatch in the horizontal beam size. The transverse *x-y* profiles are shown for a slice of the beam in (a) the bunch head and (b) the bunch tail. The values of $k_\beta s$ indicated are modulo π.

trailing slice has the same *x-y* profile as the leading slice when $k_\beta s$ (modulo π) = 0 or $\pi/2$, but looks very different at intermediate times. In particular, the vertical size of the leading slice is unperturbed by the wake field, but that of the trailing slice is perturbed. The polarity of the bunch tail deformation is not arbitrary. Exchanging the profiles at $k_\beta s = \pi/4$ and $k_\beta s = 3\pi/4$ in Figure 3.7(b), for example, would be incorrect.

Equation (3.94) says that if the beam is injected with a mismatched beam size, then at the end of the linac the bunch-tail size mismatch will grow by an extra factor of Υ compared with the bunch-head mismatch, where Υ is the growth parameter

$$\Upsilon = -\frac{Nr_0 W_2(z) L_0 a^2}{2k_\beta \gamma L}. \tag{3.95}$$

To control this type of quadrupole beam breakup instability, it is necessary to have $\Upsilon \ll 1$. For an accelerated beam, we have

$$\Upsilon = -\frac{Nr_0 W_2(z) a_i^2}{2k_\beta \gamma_i \alpha L}, \tag{3.96}$$

where a_i and γ_i are quantities taken at the injection point.

Exercise 3.14 One could BNS damp the wake induced beam size oscillation (3.94) by introducing extra focusing in the bunch tail. For a coasting beam, show that this requires

$$\Delta k_\beta = -\frac{Nr_0 W_2(z)a^2}{4k_\beta \gamma L}. \tag{3.97}$$

Figure 3.8 gives the results of a numerical simulation of the beam size of a Gaussian beam with intensity $N = 5 \times 10^{10}$ being accelerated from 42 MeV to 1.2 GeV in the first section of the SLAC linac of length 112 m. Eleven slices, evenly spaced longitudinally over a span of $4\sigma_z = 4$ mm, are used to model the bunch. In the simulation, the beam is assumed to be injected on axis, so that no dipole ($m = 1$) wake fields are generated. The longitudinal ($m = 0$) wake is included, although most of its effect has been compensated by phasing the bunch center 15° ahead of the accelerating rf voltage. The

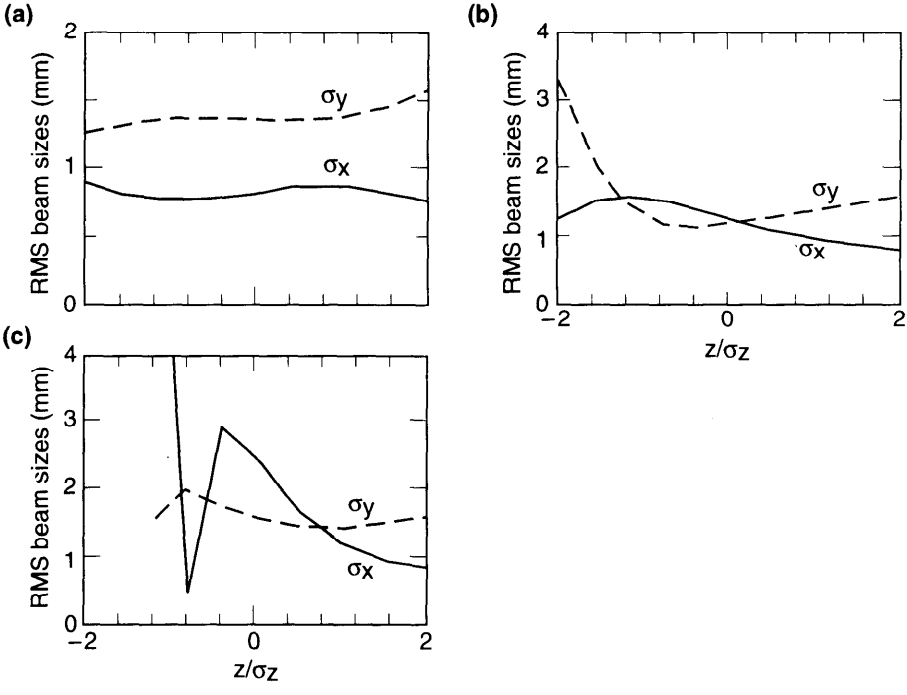

Figure 3.8. Results of a numerical simulation that demonstrates the effect of a quadrupole beam breakup in a linac. (a) The rms horizontal and vertical beam sizes along the bunch at the end of the linac section when only the $m = 0$ wake is included. (b) Same as (a), but including the $m = 2$ wake due to the FODO structure of the linac lattice. (c) The beam contains an additional quadrupole moment due to a 20% injection mismatch. In all cases, $z > 0$ is toward the head of the bunch.

slight variation of the beam sizes along the bunch in Figure 3.8(a) results from the slight energy variation along the bunch due to the $m = 0$ wake. When the quadrupole wake due to the FODO nature of the linac lattice is included, Figure 3.8(b) shows clearly that the bunch tail is perturbed. When the beam is further assumed to be injected with a 20% mismatch in σ_x and -20% in σ_x', the quadrupole beam breakup is much enhanced, as seen in Figure 3.8(c).[20]

Analysis similar to the above can be extended to higher multipole wake fields ($m > 2$). For instance, the $m = 3$ case requires the consideration of triangularly shaped charge slices. We then obtain a growth parameter Υ that resembles Eqs. (3.25) and (3.38) for $m = 1$, and Eqs. (3.95–3.96) for $m = 2$:

$$\Upsilon = -\frac{Nr_0 W_m(z)}{4k_\beta L}\begin{cases} mL_0 a^{2(m-1)}/\gamma & \text{coasting beam,} \\ ma_i^{2(m-1)}/(m-1)\alpha\gamma_i & \text{accelerated beam.} \end{cases} \tag{3.98}$$

As m increases, the growth parameter decreases roughly as $a^{2(m-1)}/b^{2m}$, where a is the transverse beam size and b is the pipe radius.

[20]Alexander W. Chao and Richard K. Cooper, Part. Accel. **13**, 1 (1983).